JOURNAL OF MATERIALS SCIENCE **34** (1999) 2979–2985

Electrical and elastic properties of conductor-polymer composites

Y. ISHIGURE, S. IIJIMA, H. ITO, T. OTA, H. UNUMA, M. TAKAHASHI, Y. HIKICHI
Ceramics Research Laboratory, Nagoya Institute of Technology, Tajimi, Japan

H. SUZUKI
Department of Materials Science, Shizuoka University, Hamamatsu, Japan
E-mail: ota@crl.nitech.ac.jp

Several series of conductor-polymer composites were prepared from metal, graphite and conducting ceramics as filler materials, and epoxy, silicone rubber, polyethylene and polypropylene as polymer matrix. Their percolation curves, pressure dependence of resistivity, and Young's modulus were examined for applications such as a pressure sensor.

1. Introduction

In the past several years, some composites containing dispersed conducting particles in an insulating polymer matrix have been studied for applications such as thermistors and pressure sensors [1–7]. The electrical resistivity of such a composite depends critically on the volume fraction of the conducting filler particles, and is well explained by percolation theory [8–10]. For a small volume fraction of the conducting filler particles, the resistivity of the composite is close to that of the polymer matrix. As the volume fraction of the conducting filler particles increases, the particles come into contact with one another to form the conduction paths through the composite. As a result, the resistivity drops by many orders of magnitude at a critical threshold. Once a saturation region of conducting filler particles is reached, there is a large number of conduction paths, resulting in a low resistivity.

For a composite near the critical threshold, we would expect to see a piezoresistive effect as well as a positive temperature coefficient [PTC] effect that has been already utilized for thermistors such as self-regulating heaters and overcurrent protection devices [11–14]. This piezoresistive effect is illustrated as follows. The conducting filler particles are essentially in non-contact in a composite just before the critical threshold, giving a high resistivity. As a stress is applied on the composite, the elastic polymer matrix deforms to the extent that the conducting filler particles are forced closer together to form the conduction paths, resulting in reduction of the resistivity. Consequently, the understanding of elastic properties of the composites is very important in order to design pressure sensors.

The elastic properties of composites containing randomly dispersed particles in a polymer matrix have been widely studied and explained by various theoretical models [15, 16]. However, there is only a few reports measuring both electrical resistivity and elastic properties simultaneously [17–19]. So, this paper reports the connection between these two properties.

2. Experimental

Table I shows conducting filler materials and polymers used in the present work. Sample preparation procedures are as follows: (a) Epoxy composites were prepared by stirring with Cu or Sb-doped SnO_2 filler in acetone, since epoxy resin was too viscous to mix. After the acetone was removed in air, the mixture was molded into disk ($25\,\phi \times 5$ mm) under 100 MPa and cured at 65 °C for 16 h. (b) Silicone rubber composites were prepared by hand-mixing with Cu, Ni, Sb-doped SnO_2 or $La_{0.5}Sr_{0.5}CoO_3$ filler, and with a small amount of hardener. The mixture was molded into disk ($25\,\phi \times 5$ mm) under 100 MPa and subsequently cured at 45 °C for 16 h. (c) Thermoplastic polymer composites were mixed with Sb-doped SnO_2 or graphite filler by laboplastomill at 140 °C for polyethylene and at 180 °C for polypropylene. The mixture was molded into disk ($25\,\phi \times 10$ mm) under 20 MPa at 140 °C for polyethylene, and under 100 MPa at 160 °C for polypropylene.

Resistance measurement was conducted by the two-point method using a LCR meter (YHP 4284A), where an air-dried silver paste was applied on polished surfaces of specimens as electrode. Piezoresistivity was measured under uniaxial pressures. Young's modulus (E) was calculated from data on the tension side of 3-point bending by using the following equation:

$$E = L^3 \cdot P/4w \cdot t^3 \cdot \delta \qquad (1)$$

where L is a span length (20 mm), w is a width, t is a thickness, P is an applied load, δ is a displacement, and a cross head speed is 0.3 mm/s. The microstructures of composites were observed by SEM (JEOL JSM-T20 and JSM-6100).

TABLE I Filler and matrix materials used in the present work

Materials (Manufacturer)	Particle size (μm)	Particle shape	Density (g/cm^3)	Resistivity ($\Omega \cdot$ cm)	Young's modulus (MPa)
Filler materials	5	Somewhat dendritic	8.69	1.7×10^{-6}	1.3×10^5
Fine Cu metal (Wako Pure Chemical Industries)					
Coarse Cu metal (Kojundo Chemical Laboratory)	<74	Dendrite	8.69	1.7×10^{-6}	1.3×10^5
Ni metal (Alfa Product)	2.5–3.0	Aggregated spherical	8.90	6.8×10^{-6}	2.1×10^5
Fine graphite (Nihon Carbon, GA-5)	<44	Plate-like	2.26	7.0×10^{-2}	ca 1×10^4
Coarse graphite (Nihon Carbon, GA-2)	150–600	Plate-like	2.26	7.0×10^{-2}	ca 1×10^4
Fine Sb-doped SnO_2 (Mitsubishi Metal, T-1)	<0.1	Spherical	6.6	1–5	ca 2×10^5
Coarse Sb-doped SnO_2 (by solid state reaction)	ca 0.5	Spherical	6.6	30–60	ca 2×10^5
$La_{0.5}Sr_{0.5}CoO_3$ (by solid state reaction)	ca 7	Angular	6.51	5–10	ca 2×10^5
Matrix materials					
Epoxy resin (A) (Oken Shoji, epok 812-DDSA)			1.20		1.2×10^3
Epoxy resin (B) (Oken Shoji, epok 812-MNA)			1.13		9.7×10^2
Silicone rubber (Toshiba Silicone, TSE 350)			1.16		1.3
Polyethylene (Ube Kosan, UM 8300)			0.92		1×10^2
Polypropylene (Idemitsu Petroleum, J-700G)			0.90		1.8×10^3

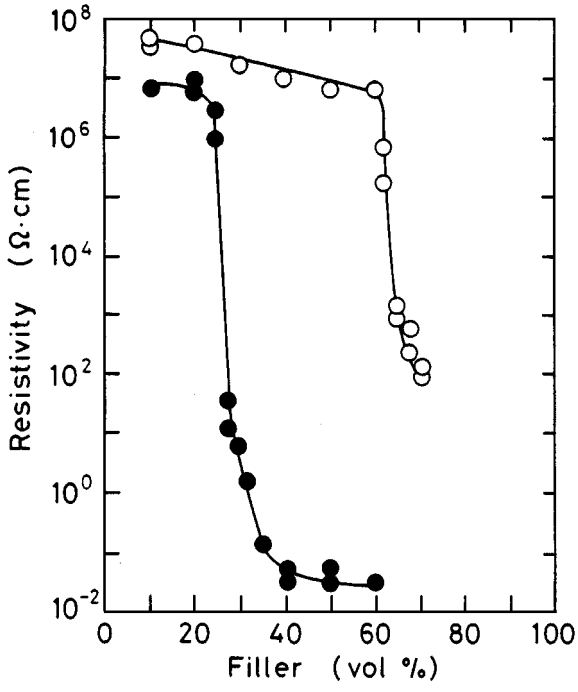

Figure 1 Electrical resistivity of fine Cu-epoxy resin composites (●) and $La_{0.5}Sr_{0.5}CoO_3$-silicone rubber composites (○) plotted as a function of conducting filler content.

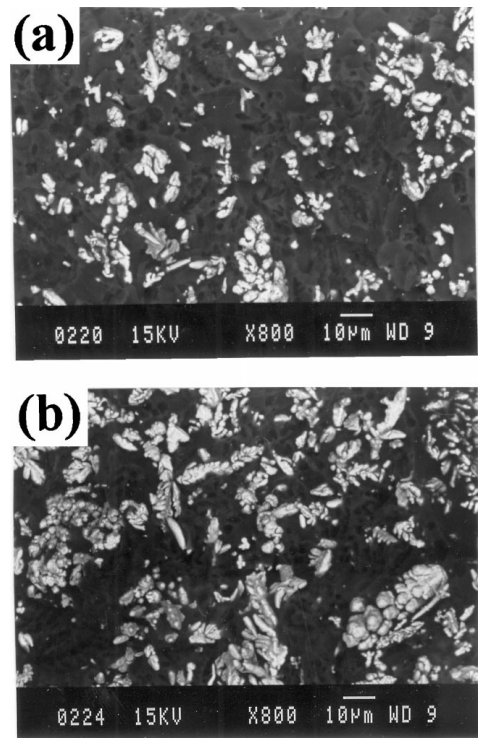

Figure 2 SEM micrographs of fine Cu-epoxy composites with (a) 25 and (b) 30 vol % loadings.

3. Results and discussion

Fig. 1 shows the typical percolation curves of conductor-polymer composites: fine Cu powder-epoxy resin and $La_{0.5}Sr_{0.5}CoO_3$-silicone rubber. Their composites had the critical thresholds at about 25 and 60 vol %, respectively. Fig. 2 shows SEM micrographs of Cu-epoxy composites. Two-dimensionally, Cu particles were isolated from one another at the critical threshold of 25 vol % (Fig. 2a), while they were considerably in contact with one another at 30 vol % in the saturation region (Fig. 2b). Fig. 3 shows the change of resistance in several samples with different powder loadings near the critical threshold as a function of pressure. In both

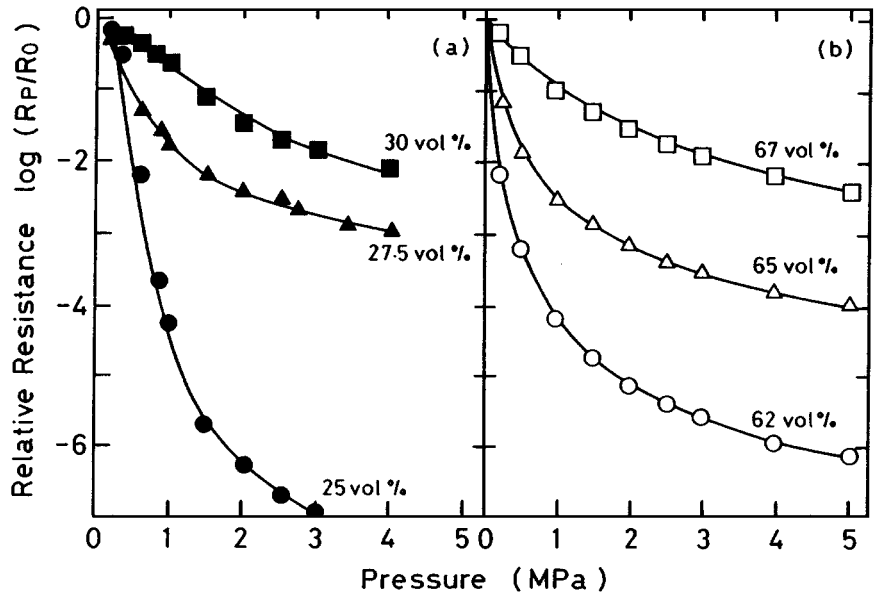

Figure 3 Pressure dependence of the electrical resistance of (a) fine Cu-epoxy resin composites and (b) $La_{0.5}Sr_{0.5}CoO_3$-silicone rubber composites.

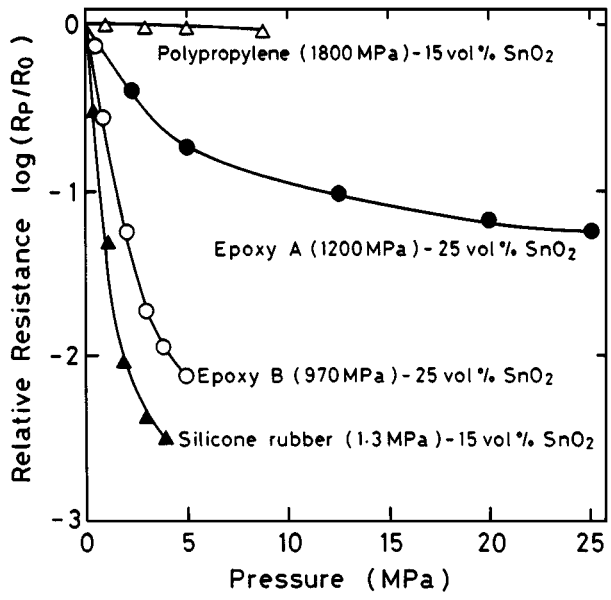

Figure 4 Pressure dependence the electrical resistance of epoxy resin A (●), epoxy resin B (○), silicone rubber (▲) and polypropylene (△) composites loaded with fine Sb-doped SnO_2 particles.

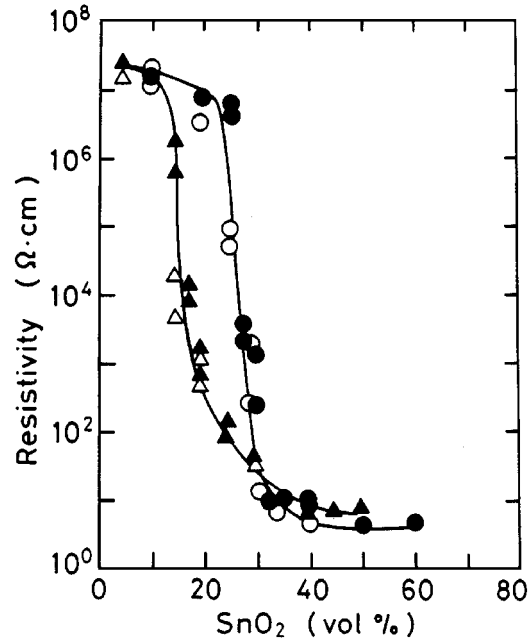

Figure 5 Electrical resistivity of epoxy resin A (●), epoxy resin B (○), silicone rubber (▲) and polypropylene (△) composites loaded with fine Sb-doped SnO_2 particles as a function of conducting filler content.

composites, the samples closer to their critical thresholds showed larger changes of resistance. This large piezoresistive effect was thought to be caused by a higher resistivity under no pressure and by a lower Young's modulus of the composites.

Fig. 4 shows the piezoresistive effect of some composites near critical thresholds. Fig. 5 shows their percolation curves. These composites were prepared by loading SnO_2 particles in two kinds of epoxy resin (A: 1200 MPa, B: 970 MPa), propyropylene (1800 MPa) and silicone rubber (1.3 MPa) with different Young's moduli. Fig. 6 shows SEM micrographs of the composites near their critical thresholds shown in Fig. 4. SnO_2 particles were buried in polymer matrix under the almost same situation for every composite. By comparing the pressure dependence of the electrical resistance of two kinds of epoxy resin composites with 25 vol % SnO_2 loadings, or polypropylene and silicone rubber composites with 15 vol % SnO_2 loadings, it is evident that the composites prepared from polymer matrix having a lower Young's modulus revealed a larger piezoresistive effect.

Figs 7–10 show the changes of electrical resistivity, Young's modulus and torque at mixing as a function of the volume fraction of the conducting filler in the following composites: Cu and Ni metal-silicone rubber (Fig. 7); SnO_2 and $La_{0.5}Sr_{0.5}CoO_3$-silicone rubber (Fig. 8); SnO_2-polyethylene (Fig. 9); graphite-polyethylene (Fig. 10). In each series of the composites, the changes of resistivity showed the so-called percolation curves as shown in Figs 7a, 8a, 9a and 10a. On the other hand, the Young's modulus showed the

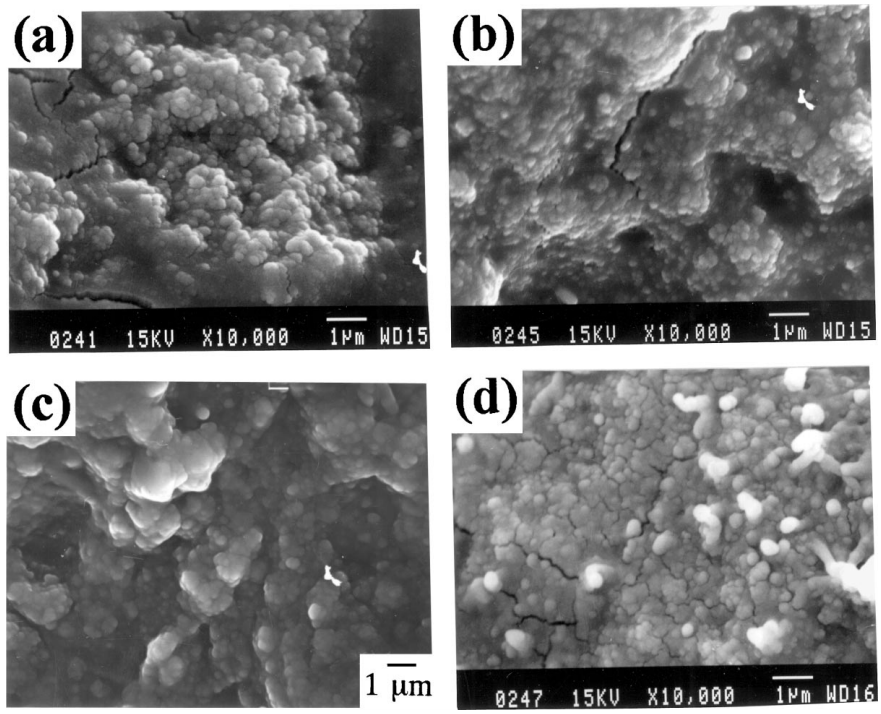

Figure 6 SEM micrographs of (a) epoxy resin A (25 vol %), (b) epoxy resin B (25 vol %), (c) silicone rubber (15 vol %) and (d) polypropylene (15 vol %) composites loaded with fine Sb-doped SnO_2 particles.

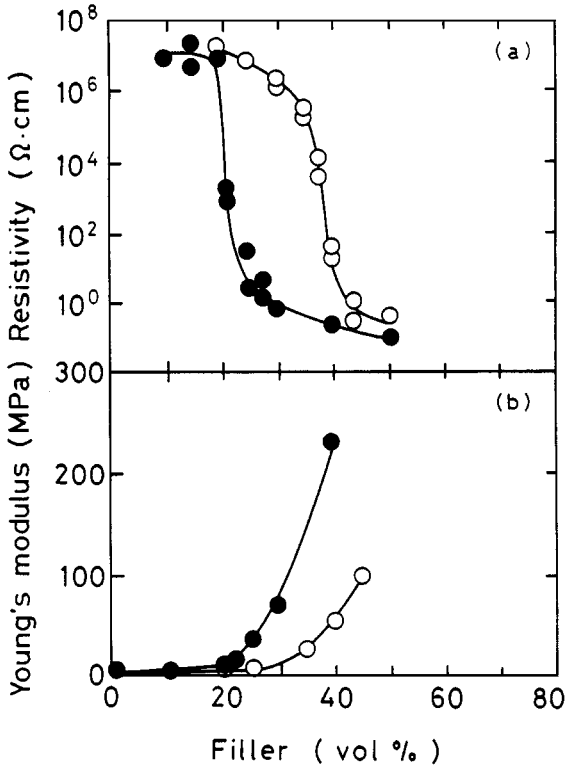

Figure 7 (a) Electrical resistivity and (b) Young's modulus of coarse Cu (○) and Ni (●)-silicone rubber composites plotted as a function of conducting filler content.

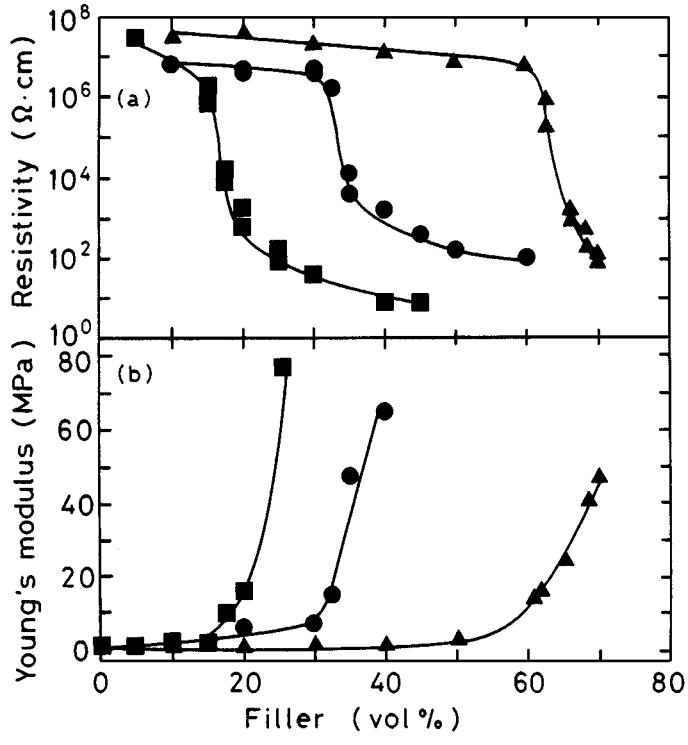

Figure 8 (a) Electrical resistivity and (b) Young's modulus of fine (■) and coarse (●) Sb-doped SnO_2 and $La_{0.5}Sr_{0.5}CoO_3$ (▲)-silicone rubber composites plotted as a function of conducting filler content.

just reversed change of resistivity as shown in Figs 7b, 8b, 9b and 10b. For a small volume fraction of filler, Young's modulus was closer to that of the continuous polymer matrix. When the volume fraction of filler increased up to the critical threshold, the resistivity started to decrease, while Young's modulus started to increase. After the percolation curve reached a saturation region by an additional increase of filler, Young's modulus increased steeply. In a similar manner as the change of Young's modulus, the torque at mixing of graphite-polyethylene composites also showed a larger inclination in the saturation region as shown in Fig. 10c.

It was thought that the increase of Young's modulus was caused mainly by the contact of particles with one another. This is because, the filler particle's moduli

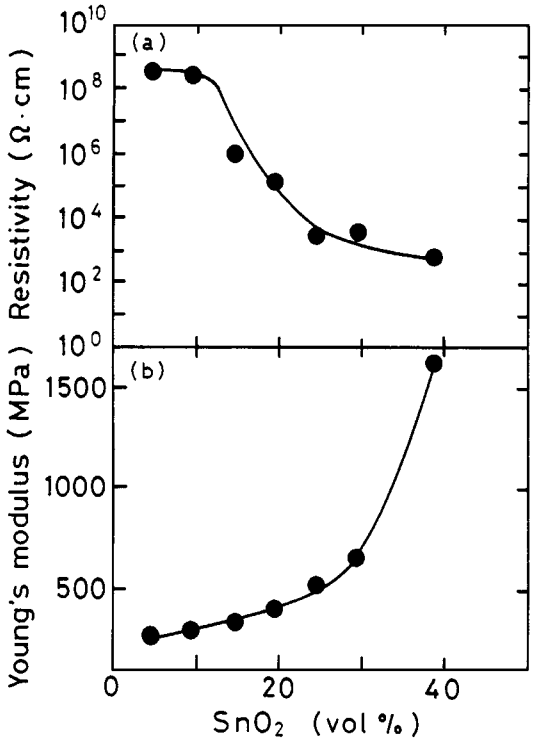

Figure 9 (a) Electrical resistivity and (b) Young's modulus of coarse Sb-doped SnO_2-polyethylene composites plotted as a function of conducting filler content.

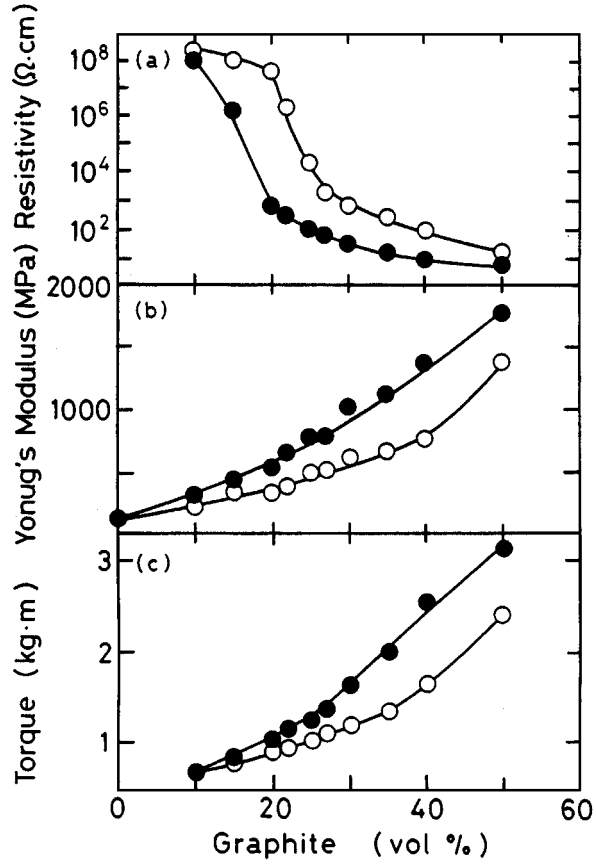

Figure 10 (a) Electrical resistivity, (b) Young's modulus and (c) torque at mixing of fine (●) and coarse (○) graphite-polyethylene composites plotted as a function of conducting filler content.

are bigger than those of polymer matrices. Figs 11–13 show SEM micrographs of Ni-silicone rubber, coarse SnO_2-silicone rubber and fine SnO_2-polyethylene composites, respectively. Up to critical threshold, Young's modulus as well as electrical resistivity of composites showed only a small variation, since the filler particles were isolated and buried in polymer matrix as shown in Figs 11a, 12a,b, and 13a. When the volume fraction of filler just exceeded the critical threshold, the contact between particles arose. As a result, the resistivity abruptly dropped with the conduction paths formed by the minor contact between particles, as shown in Figs 11b, 12c and 13b. On the other hand, the Young's modulus remained almost unchanged with the major part of isolated particles in the continuous polymer matrix. When most of particles came into contact with one another in the saturation region as shown in Figs 11d, 12d and 13c,d, the electrical resistivity showed a small variation, while the Young's modulus increased so significantly with increasing volume fraction of filler. Accordingly, it was concluded that the change of elastic property such a Young's modulus lagged behind that of electrical resistivity.

In addition, it is known that the percolation curve is greatly affected by size of conducting filler particles, and that it shifts to the low fraction side with decreasing particle size [7, 20, 21]. Consistent with these observations, the percolation curves of resistivity shifted to the low volume fraction side with decreasing particle size in the present work. Equally, the curves of Young's modulus also shifted to the low volume fraction side with decreasing particle size in agreement with the percolation curves of resistivity as shown in Figs 7–10. In order to predict elastic modulus as a function of volume fraction of filler, there have been a number of theoretical approaches such as the mixture rule, the Hashin-Shtrikman type predictions and so on [15, 16]. Their expressions were derived for upper and lower bounds on the elastic properties of two-phase systems. Generally, the simplest case is the mixture rule. The upper and lower bounds are calculated from Equations 2 and 3 as the series and parallel models, respectively:

$$E_c = E_f v_f + E_m v_m \quad (2)$$

$$E_c = (v_f/E_f + v_m/E_m)^{-1} \quad (3)$$

where E_c, E_f and E_m are Young's modulus for composite, filler and matrix, and v_f and v_m are the volume fraction of filler and matrix, respectively. In most cases, the bounds predicted after Hashin and Shtrikman or Ravichandran are much closer to experimental data than those predicted by the mixture rule [16]. The experimental curves of Young's modulus in the present work roughly varied along the lower bound for parallel model or the upper bounds after Ravichandran up to the critical threshold, and then increased steeply toward the upper bound for series model beyond the critical threshold. This behavior could not be explained by any presented theoretical expressions, since there is little approach to effect of filler size on elastic properties of composites. However, a work has been done for an aspect ratio of filler [15]. For spherical filler, the well known Kerner's equation predicts the curve along the parallel model, Equation 3. When the aspect ratio increases, Young's

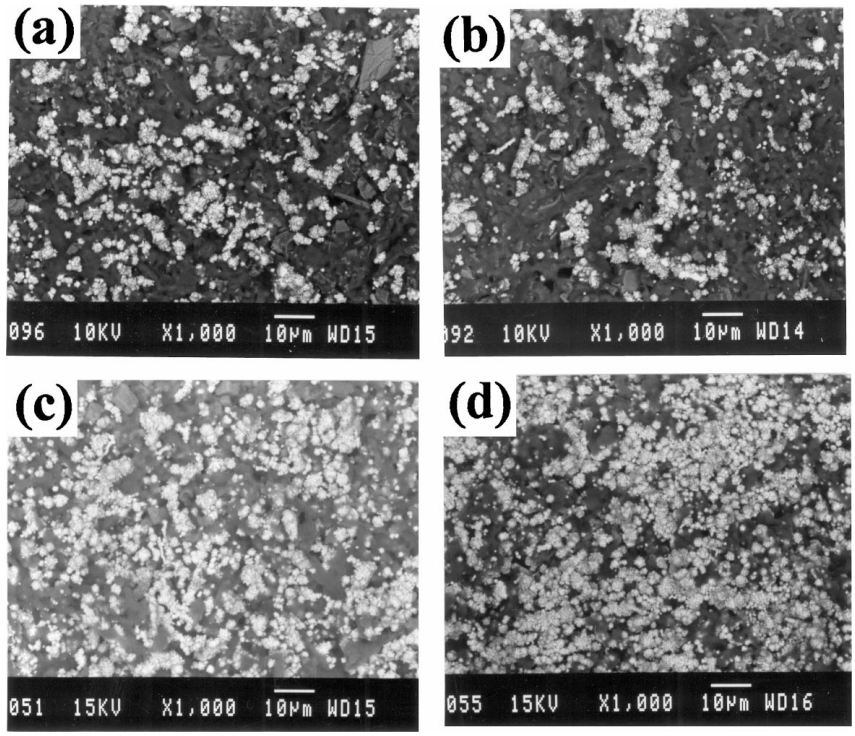

Figure 11 SEM micrographs of Ni-silicone rubber composites with (a) 20, (b) 22, (c) 30 and (d) 40 vol % loadings.

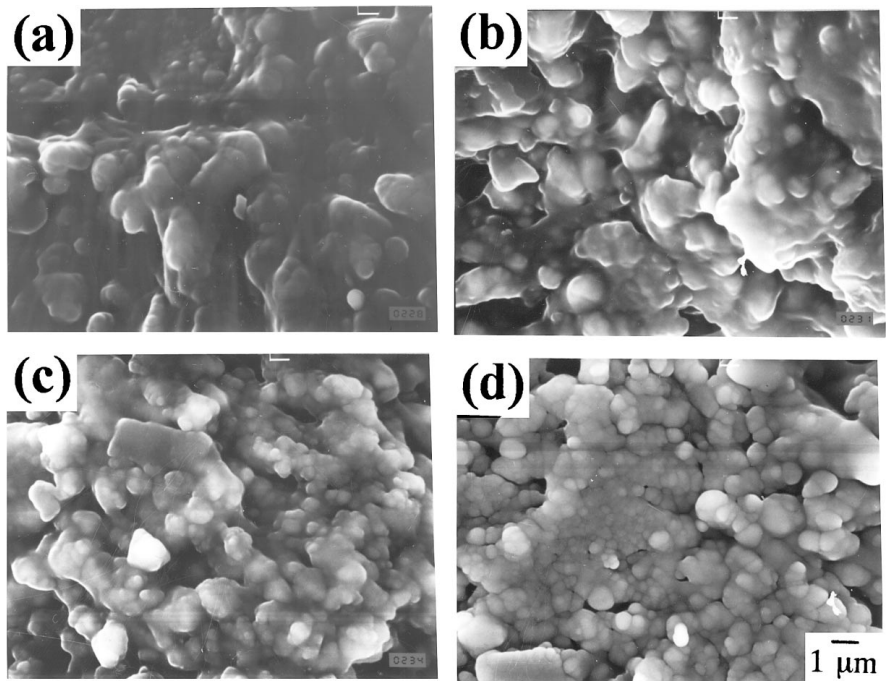

Figure 12 SEM micrographs of coarse SnO_2-silicone rubber composites with (a) 20, (b) 30, (c) 33 and (d) 40 vol % loadings.

modulus gradually approaches the series model, Equation 2. The filler particles come into contact with one another to form the conduction paths beyond the critical threshold. Consequently, it was thought that these paths must function as a continuous fibrous filler, and then Young's modulus steeply increased toward the upper bound for series model.

4. Summary

Some conductor-polymer composites showed a piezoresistive effect near the critical threshold of the percolation curve. This effect was large in composites prepared from polymers such a silicone rubber having a low Young's modulus. The changes of the electrical resistivity and Young's modulus as function of the volume fraction of conducting filler were correlated to each other. For a small volume fraction of filler, both electrical resistivity and Young's modulus were closer to those of the continuous polymer matrix. When the volume fraction of filler increased, the electrical resistivity abruptly droped at the critical threshold, while Young's modulus increased steeply in a saturation region beyond the critical threshold. That is to say, the change

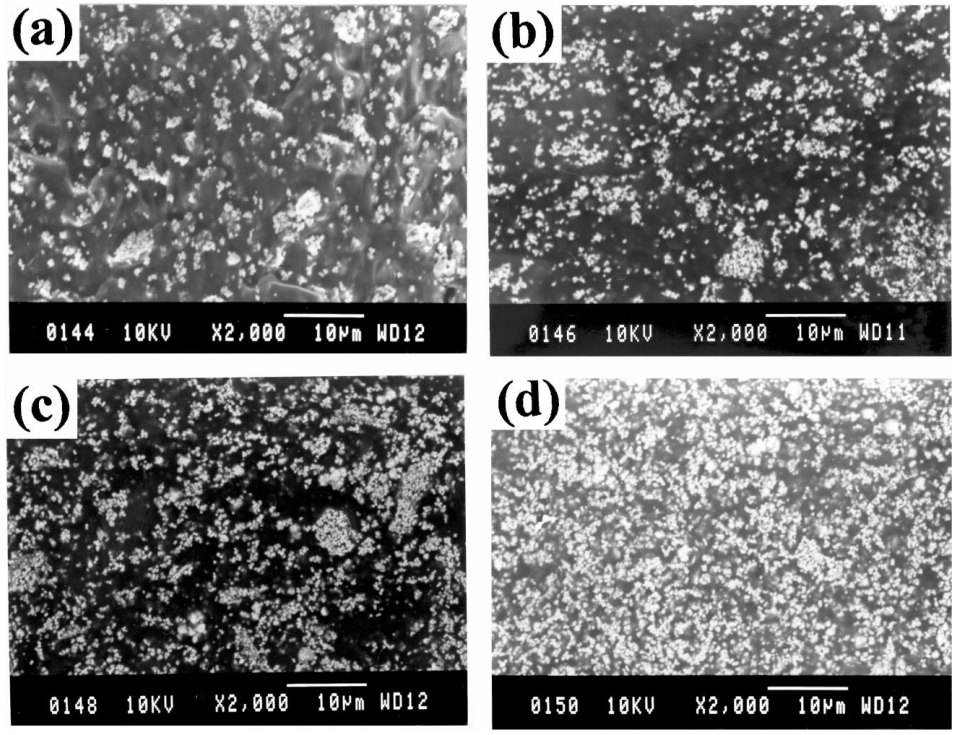

Figure 13 SEM micrographs of fine SnO_2-polyethylene composites with (a) 10, (b) 20, (c) 30 and (d) 40 vol % loadings.

of Young's modulus lagged behind that of resistivity. This would be of benefit to pressure sensors having a high resistivity and a low Young's modulus. However, Young's modulus measured in this study depended on tension, while the resistivity in pressure sensors should depend on compression. Consequently, further experimental work is in progress to understand more clearly the relation between the electrical and elastic properties in conductor-polymer composites.

References

1. K. A. HU, D. MOFFATT, J. RUNT, A. SAFARI and R. NEWNHAM, *J. Amer. Ceram. Soc.* **70** (1987) 583.
2. D. MOFFATT, J. RUNT, A. HALLIYAL and R. NEWNHAM, *J. Mater. Sci.* **24** (1989) 609.
3. L. ROHLFING, R. NEWNHAM, S. PILGRIM and J. RUNT, *J. Wave-Mater. Interaction* **3** (1988) 273.
4. K. YOON and Y. NAM, *J. Mater. Sci.* **27** (1992) 4051.
5. F. CARMONA, R. CANET and P. DELHAES, *J. Appl. Phys.* **61** (1987) 2550.
6. S. YOSHIKAWA, T. OTA, R. NEWNHAM and A. AMIN, *J. Amer. Ceram. Soc.* **73** (1990) 263.
7. T. OTA, I. YAMAI, J. TAKAHASHI, R. NEWNHAM and S. YOSHIKAWA, *Ceram. Trans.* **19** (1991) 381.
8. D. MCLACHLAN, M. BLASZKIEWICZ and R. NEWNHAM, *J. Amer. Ceram. Soc.* **73** (1990) 2187.
9. S. KIRKPATRIK, *Rev. Mod. Phys.* **45** (1973) 574.
10. F. LUX, *J. Mater. Sci.* **28** (1993) 285.
11. J. MEYER, *Polym. Eng. Sci.* **13** (1973) 462.
12. M. NARKIS and A. VAXMAN, *J. Appl. Polym. Sci.* **29** (1984) 1639.
13. F. DOLJACK, *IEEE CHMT-4* (1981) 372.
14. R. SHERMAN, L. MIDDLEMAN and S. JACOBS, *Polym. Eng. Sci.* **23** (1983) 36.
15. T. S. CHOW, *J. Mater. Sci.* **15** (1980) 1873.
16. K. S. RAVICHANDRAN, *J. Amer. Ceram. Soc.* **77** (1994) 1178.
17. S. K. BHATTACHARYYA, S. K. DE and S. BASU, *Polym. Eng. Sci.* **19** (1979) 533.
18. N. DEPREZ, D. S. MCLACHLAN and I. SIGALAS, *Solid State Commun.* **66** (1988) 869.
19. P. K. PRAMANIK, D. KHASTAGIR and T. H. SAHA, *J. Mater. Sci.* **28** (1993) 3539.
20. R. P. KUSY, *J. Appl. Phys.* **48** (1977) 5301.
21. K. MORI, Y. OKAI, H. YAMADA and Y. KASHIWABA, *J. Mater. Sci.* **28** (1993) 367.

Received 7 February 1997
and accepted 22 January 1999